

Dietary Oxalate Induces Urinary Nanocrystals in Humans



Parveen Kumar¹, Mikita Patel¹, Vinoy Thomas², John Knight¹, Ross P. Holmes¹ and Tanecia Mitchell¹

¹Department of Urology, University of Alabama at Birmingham, Birmingham, Alabama, USA; and ²Department of Materials Science and Engineering, University of Alabama at Birmingham, Birmingham, Alabama, USA

Introduction: Crystalluria is thought to be associated with kidney stone formation and can occur when urine becomes supersaturated with calcium, oxalate, and phosphate. The principal method used to identify urinary crystals is microscopy, with or without a polarized light source. This method can detect crystals above 1 μm in diameter (microcrystals). However, analyses of calcium oxalate kidney stones have indicated that crystallite components in these calculi are 50–100 nm in diameter. Recent studies have suggested that nanocrystals (<200 nm) elicit more injury to renal cells compared to microcrystals. The purpose of this study was to determine whether (i) urinary nanocrystals can be detected and quantified by nanoparticle tracking analysis (NTA, a high-resolution imaging technology), (ii) early-void urine samples from healthy subjects contain calcium nanocrystals, and (iii) a dietary oxalate load increases urinary nanocrystal formation.

Methods: Healthy subjects consumed a controlled low-oxalate diet for 3 days before a dietary oxalate load. Urinary crystals were isolated by centrifugation and assessed using NTA before and 5 hours after the oxalate load. The morphology and chemical composition of crystals was assessed using electron microscopy, Fourier-transform infrared spectroscopy (FTIR), and ion chromatography-mass spectrometry (IC-MS).

Results: Urinary calcium oxalate nanocrystals were detected in pre-load samples and increased substantially following the oxalate load.

Conclusion: These findings indicate that NTA can quantify urinary nanocrystals and that meals rich in oxalate can promote nanocrystalluria. NTA should provide valuable insight about the role of nanocrystals in kidney stone formation.

Kidney Int Rep (2020) 5, 1040–1051; <https://doi.org/10.1016/j.ekir.2020.04.029>

KEYWORDS: crystalluria; kidney stones, nanoparticle tracking analysis; oxalate

© 2020 International Society of Nephrology. Published by Elsevier Inc. This is an open access article under the CC BY-NC-ND license (<http://creativecommons.org/licenses/by-nc-nd/4.0/>).

Urine can be supersaturated with minerals such as calcium, oxalate, and phosphate that are derived from dietary sources or endogenous metabolism.^{1–3} The interaction and binding of these minerals with each other can result in the formation of urinary crystals. Several lines of evidence have established that the majority of calcium oxalate (CaOx) kidney stones form when CaOx crystals deposit on Randall's plaques or plugs of ducts of Bellini.^{4–6} Crystallites appear to be the building blocks of such stones and are sub-micron in size (50–100 nm in diameter), as characterized by atomic force microscopy, electron microscopy, and

X-ray diffraction.^{7,8} Conventional methods currently available to detect and characterize crystals that are excreted in urine include polarized light microscopy, scanning electron microscopy, urine filtration, evaporation, and centrifugation.^{9–15} Several research groups have suggested that the degree of crystalluria is positively correlated with kidney stone risk in stone formers^{9,13} and individuals with metabolic disorders.¹⁶ Recently, Daudon *et al.* proposed that crystalluria predicts kidney stone recurrence and could potentially be useful in assessing responses to preventive therapy.¹⁷ We have previously shown that dietary oxalate loads substantially increase plasma oxalate and urinary oxalate excretion in normal subjects and stone formers.^{18,19} Whether crystalluria accompanies these surges in oxalate excretion was not established.

Increased urine supersaturation with stone-forming components is thought to augment crystal binding to

Correspondence: Tanecia Mitchell, Department of Urology, University of Alabama at Birmingham, Hugh Kaul Human Genetics Building, 816E, 720 20th Street South, Birmingham, AL 35294. E-mail: taneciamitchell@uabmc.edu

Received 26 February 2020; revised 9 April 2020; accepted 27 April 2020; published online 7 May 2020

the nidus of a stone and promote stone growth.^{20–22} Both CaOx (monohydrate and dihydrate) and brushite crystals in stones have been identified to be 60–100 nm in size using powder X-ray diffraction; however, hydroxyapatite crystals appear to be significantly smaller (15 nm).²⁰ It has also been reported in a separate study, using atomic force microscopy, that these small particles are between 50 and 280 nm.²³ The presence of such crystals could be a potential source of epithelial cell inflammation.²⁴ Recently, it was reported that nanocrystals cause more organelle injury and apoptosis to cultured renal cells than crystals larger than 1 μm , and their effects can vary based on crystal shape and size.²⁵ These findings suggest that nanocrystals may play an important role in stone growth and cause cellular injury and oxidative stress, which may further drive stone formation.²⁶ Thus, the ability to accurately identify and quantify nanocrystals could help further define important events in kidney stone formation.

Currently, there are no well-established methods that can measure both the size and numbers of urinary nanocrystals. Previous investigations have used a range of instruments including a nanoscale flow cytometer, a Zetasizer Nano-ZS with an X-ray diffractometer, and fluorescently labeled bisphosphonate probes to evaluate urinary nanocrystals.^{27,28} Limitations of these approaches include the inability to quantify the number of nanocrystals present, the use of nonspecific fluorescent probes, and the need for extensive sample preparation. The purpose of this study was to determine whether (i) urinary nanocrystals can be detected and quantified by NTA (a high-resolution imaging technology), (ii) early void urine samples contain calcium nanocrystals, and (iii) a dietary oxalate load increases urinary nanocrystal formation in healthy subjects. NTA measures nanoparticles in solution based on Brownian motion using a laser.²⁹ NTA has been used in a number of studies to assess particle size and enumerate nanoparticles, such as exosomes, liposomes, microspheres, and vesicles in a variety of biological samples including blood, breast milk, and urine.^{30–33} Additionally, implementation of fluorescent filters, fluorescent dyes, and antibodies can enhance the specificity of NTA.³⁴ Fluo-4 is a fluorescent dye that has been used previously to detect calcium-containing particles in human synovial fluid using flow cytometry and fluorescent microscopy.³⁵ We therefore assessed whether fluorescent calcium-binding dyes could also be used to assess urinary nanocrystals by NTA. Our findings show that both micro- and nano-sized urinary crystals can be detected before and following a single dietary oxalate load. As NTA can efficiently and specifically detect

calcium-containing nanocrystals in human urine, it should be a useful tool for increasing our understanding of kidney stone formation and growth.

METHODS

Reagents

CaOx monohydrate crystals were synthesized by adding sodium oxalate (1 mM) to CaCl_2 (10 mM) in HEPES/NaCl solution.³⁶ The mixture was vortexed for 1 minute and allowed to stand undisturbed for 72 hours. Subsequently, the liquid layer was removed without disturbing the crystal layer. CaOx crystals were collected and underwent a series of centrifugations to remove all liquid. Lastly, the pellet was air dried inside the hood for 2 days prior to weighing and visualizing under a polarized light microscope. The concentration of oxalate in the crystals was determined using IC-MS.³⁷ Calcium phosphate (CaP; hydroxyapatite) crystals, Calcium green (hexapotassium salt), Fluo-4 pentapotassium salt (Fluo-4), and gold nanoparticles were all purchased from Millipore Sigma (St. Louis, MO). Fluo-4 AM and Calcein Ultragreen AM were purchased from AAT Bioquest (Sunnyvale, CA).

Clinical Protocol and Urine Collection

This research was approved by the University of Alabama at Birmingham (UAB) Institutional Review Board and was in accordance with the Helsinki declaration. Additionally, this work is registered under clinicaltrials.gov (identifier: NCT03877276). Written informed consent was obtained from all participants. Healthy adults who do not form kidney stones ($n = 14$, age 34.5 ± 9.8 years, BMI 25.2 ± 3.8 kg/m^2 , and 50% women) were recruited from the Birmingham, AL area. Diets were prepared by the CCTS Clinical Research Unit and were controlled in protein, carbohydrate, calcium, oxalate, and other nutrients.¹⁸ Diets contained 50 mg oxalate and 1000 mg calcium/2000 kcal per day. Participants consumed this low-oxalate diet for 3 days prior to fasting overnight. The following morning, participants were asked to void after waking up and consume 4 cups of water. After arriving at the clinical research unit, they provided a fasted urine sample (pre-oxalate; 2 hours after first void) that was kept at room temperature (RT) and processed within 5 minutes of collection. Next, they consumed breakfast and an 8-mmol oxalate load containing 68 mg of calcium (i.e., blended smoothie containing spinach, banana, orange juice, and avocado). After consuming the oxalate load, participants collected their urine over 5 hours (post-oxalate sample) at RT. Participants did not consume any other food and only consumed bottled water throughout this time. All urine samples were

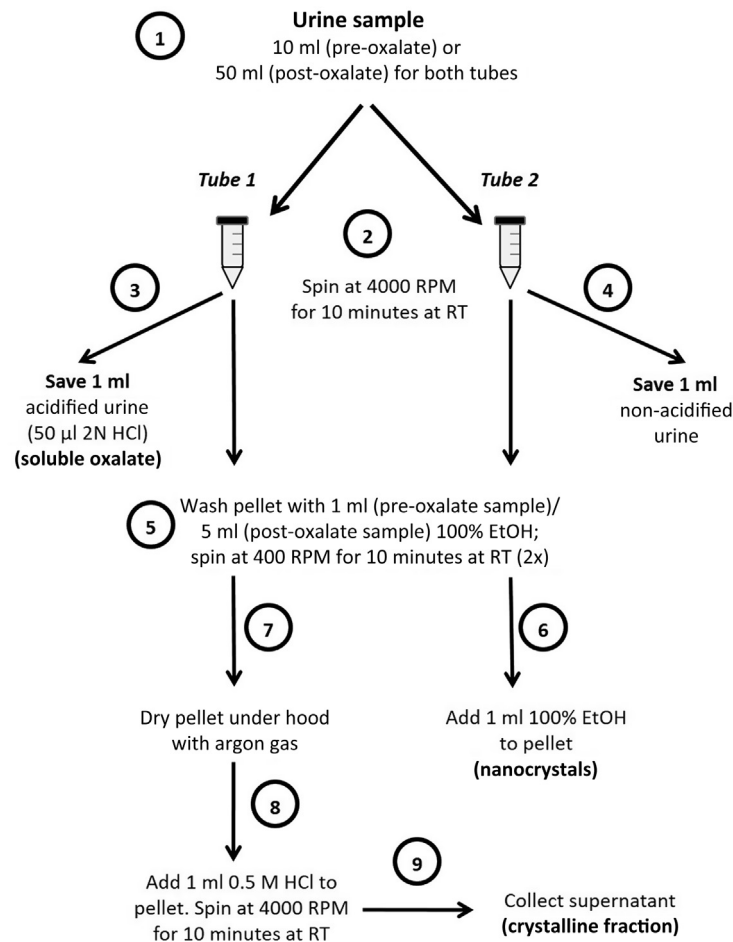


Figure 1. Flow diagram of experimental protocol to assess urinary nanocrystals. Pre-oxalate and post-oxalate urine samples were centrifuged, collected, and acidified or non-acidified for future analysis. Pellets were washed with ethanol and centrifuged prior to being either dried and acidified (crystalline fraction) or re-suspended in ethanol (nanocrystals). EtOH, absolute ethanol; HCl, hydrochloric acid; RT, room temperature.

maintained at RT and processed within 5 minutes of collection as described below.

Urine Processing

Urine pH, volume, and osmolality (Wescor Vapro Vapor Pressure Osmometer, Logan, UT) were measured prior to processing urine as shown in Step 1 of Figure 1. Following centrifugation (4000 RPM for 10 minutes at RT), aliquots of urine were acidified with 2N hydrochloric acid or not acidified (steps 2–4, Figure 1). Acidified urine samples were used to measure calcium, phosphate, and oxalate. Non-acidified urine was used to measure creatinine. Urine calcium, phosphate, and creatinine were assessed using an EasyRA chemical analyzer. IC-MS was performed to measure oxalate levels as previously described.^{37,38} Pellets harvested from urine following centrifugation were washed with absolute ethanol and centrifuged (4000 RPM for 10 minutes at RT) twice to remove traces of urine and cellular debris (Step 5, Figure 1). Pellets were either resuspended in absolute ethanol prior to NTA; Step 6) or dried with argon gas and resuspended in 0.5 M HCl

before determining oxalate, calcium, and phosphate concentrations (steps 7–9, Figure 1).

Nanoparticle Tracking Analysis

The NanoSight NS300 Instrument (Malvern Instruments, Malvern, UK), equipped with a 500 long pass Chroma Emission fluorescence filter and a 488-nm laser, was used to measure the concentration and size of urinary nanocrystals of less than 1 micron. The NanoSight platform was cleaned with air and water to ensure no residue was present and to remove any potential air bubbles prior to analyzing samples. Gold nanoparticles (100 nm in diameter, Millipore Sigma, St. Louis, MO) were diluted in water (1:1000) and included as a control to optimize and evaluate instrument settings and performance. CaOx and CaP crystals (Millipore Sigma, St. Louis, MO) were also used as controls to adjust the focus and camera settings.

CaOx and CaP crystals were diluted in water (50 µM, equivalent to 7.3 µg/ml and 25.2 µg/ml, respectively) and incubated with either Calcium Green, Fluo-4, Fluo-4 AM, or Calcein Ultragreen AM fluorescent dyes

(10 μM) for 30 minutes at RT. Calcium green and Fluo-4 are fluorescent calcium-binding dyes that are cell permeant and membrane impermeant, respectively. Fluo-4 AM is a cell-permeant calcium-binding fluorescent dye with an acetomethyl group that masks negatively charged carboxylic groups and has high chemical stability. Calcein Ultragreen AM is a cell viability marker that has properties similar to those of Fluo-4 AM. Samples were subsequently analyzed on the NanoSight to detect particles. Pre-oxalate and post-oxalate urine samples were resuspended in MilliQ water (1:10) prior to being stained with Fluo-4 AM (10 μM) for 30 minutes and analyzed on the NanoSight machine. All samples were recorded for 5 captures per sample and collected for 60 seconds using a camera level of 12. Images and videos were recorded and saved for each measurement. The flow of samples was continuously monitored to ensure the platform was not clogged. Three replicates were analyzed to ensure method and data rigor and reproducibility.

Confocal, Polarized Light, and Electron Microscopy

Microscopy was used to assess crystal morphology. All samples (CaOx and CaP crystals; pre- and post-oxalate load samples) were plated in 8-well chamber slides in Milli-Q water prior to being treated with Fluo-4 AM dye (10 μM ; 30 minutes) to image crystals. Z-stack images were collected using a Zeiss LSM 710 spectral confocal laser scanning microscope (Carl Zeiss Microscopy, GmbH, Jena, Germany) and analyzed using Zen 2.3 Lite software (Carl Zeiss AG, Oberkochen, Germany). In additional experiments, polarized light microscopy was used to identify birefringent crystals. Samples (50 μl) were placed on glass microscope slides and covered with coverslips and viewed under polarized light using an Olympus BX51 microscope with QIMAGINE RETIGA camera. Images were captured using Bioquant Imagine Analysis software (Nashville, TN). Crystalluria was further assessed using electron microscopy.³⁹ Samples (3 μl) were applied to glow-discharged 400-mesh, carbon-only copper grids (Electron Microscopy Sciences, Hatfield, PA) and allowed to air dry. The unstained grids were imaged on a FEI Tecnai F20 electron microscope (Eindhoven, Netherlands) operated at 200 kV with nominal magnifications between 10,600 \times and 15,200 \times . Images were collected on a Gatan K2 direct electron detector.

Nanocrystal FTIR Analysis

FTIR was used to confirm composites (i.e., calcium, oxalate, and phosphate) in CaOx and CaP crystals and human urinary crystal samples. Background correction was applied before sample analysis. A small volume of

Table 1. Urine chemistries of study participants

	Pre-oxalate	Post-oxalate
Volume (ml)	79.8 \pm 8.7	907.9 \pm 147.9
pH	6.3 \pm 0.1	7.1 \pm 0.1
Osmolality (mOSM/kg)	419.4 \pm 71.1	286.3 \pm 58.8
Creatinine (g)	0.08 \pm 0.02	0.24 \pm 0.04
Oxalate (mg)	5.05 \pm 2.6	33.3 \pm 4.9
Calcium (mg)	4.4 \pm 1.5	13.5 \pm 3.6
Phosphate (mg)	18.9 \pm 7.5	41.8 \pm 8.0
Oxalate/creatinine (mg/g)	19.6 \pm 3.1	117.6 \pm 18.9

Data are presented as mean \pm SEM.

concentrated sample (10 μl) was placed on the diamond window of the FTIR spectrometer (Thermo Scientific Instruments, Waltham, MA) sensor to collect the spectrum under attenuated total reflectance mode. Spectra were collected on 64 scans per sample in the range of 400–4000 cm^{-1} .

Nanocrystal Analytic Methods

The amount of calcium and phosphate present in urinary nanocrystals was determined by IC with suppressed conductivity detection (Thermo Fisher Scientific Inc., Waltham, MA). Phosphate was measured using an AS11-HC-4 μm , 2 \times 250 mm, anion exchange hydroxide, as previously described.³⁸ Calcium was measured using a CS16-Fast-4 μm , 2 \times 150 mm, cation exchange column operated at 0.16 ml/min, at 40 $^{\circ}\text{C}$, with 30-mM methanesulfonic acid as the mobile phase.

Statistical Analysis

GraphPad Prism (version 7; La Jolla, CA) software was used for statistical analyses. All data are presented as mean \pm SE. Differences in pre-oxalate and post-oxalate samples were determined using a 2-tailed Student's *t* test. A *P* value <0.05 was considered statistically significant.

RESULTS

The Effect of a Dietary Oxalate Load on Urine Chemistries and Crystalluria

Urine was collected to evaluate urine chemistries before and after a dietary oxalate load (Table 1). Urine volume, pH, creatinine, oxalate, calcium, and phosphate levels were all elevated following the oxalate load compared to pre-oxalate samples. As expected, osmolality was decreased following the oxalate load (Table 1). The amount of oxalate in post-oxalate samples was 6-fold higher than pre-oxalate samples (19.6 \pm 3.1 mg/g creatinine pre-oxalate vs. 117.6 \pm 18.9 mg/g creatinine post-oxalate; Table 1). These values are consistent with our previous studies assessing urinary oxalate levels following a load.^{18,19} To identify whether crystals

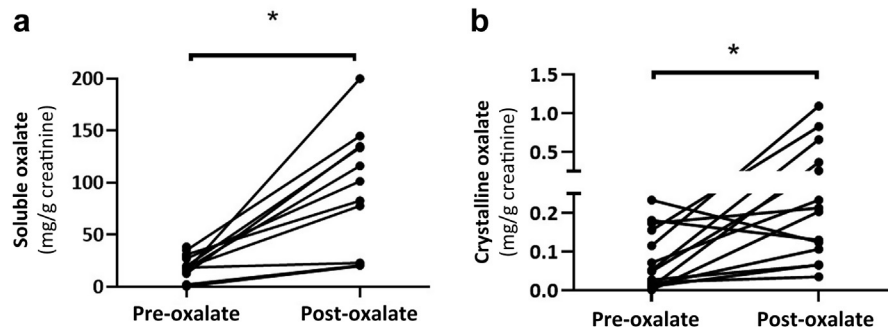


Figure 2. Urinary oxalate levels in healthy subjects following a dietary oxalate load. Ion chromatography–mass spectrometry was used to assess (a) soluble and (b) crystalline oxalate levels in healthy subjects on a controlled diet before (pre-oxalate sample) and following an oxalate load (post-oxalate sample). * $P < 0.05$.

formed with an oxalate load, urinary oxalate levels (soluble and crystalline) were assessed using IC–MS. As shown in [Figure 2a](#), soluble urinary oxalate levels were significantly increased following the oxalate load compared to pre-oxalate samples. This elevation in oxalate was also observed in crystalline fractions of the samples ([Figure 2b](#)).

NTA Detects CaOx and Calcium Phosphate (CaP) Crystals

Urinary nanocrystals were evaluated using NTA after determining that crystalline oxalate levels were elevated following an oxalate load. Fluorescent-labelled dyes that bind to calcium (Fluo-4, Calcium green, and Fluo-4 AM [Fluo-4 hydrophobic acetomethoxy]) or detect cell viability (Calcein Ultragreen AM) were evaluated for their ability to enhance the detection of calcium-containing crystals by NTA. Fluo-4 AM was the only dye that could detect CaOx crystals (50 μ M, [Supplementary Figure S1A](#)). The inability of the other dyes to stain nanocrystals could be a result of their negative charge. Based on a dose response curve using a fluorescence plate reader, a concentration of 10- μ M Fluo-4 AM produced an adequate signal-to-noise ratio ([Supplementary Figure S1B](#)). CaOx crystals were also evaluated using both fluorescence and non-fluorescence scattered light filters for NTA ([Supplementary Figure S1C](#)). The use of a fluorescence filter detected CaOx crystals in post-oxalate samples labelled with Fluo-4AM and increased specificity compared to samples detected by scattered light only. To determine whether NTA could correctly assess known concentrations of crystals, a standard curve of Fluo-4 AM-labelled CaOx crystals was generated ([Supplementary Figure S2](#)). The number of particles detected correlated with the concentration of known amounts of CaOx crystals ($R^2 = 0.94$). As shown in [Figure 3a](#), the size of CaOx crystals (50 μ M) labelled with Fluo-4 AM ranged from 75 to 300 nm (mean, 206.5 \pm 18.2 nm). Labelled CaP crystals (50 μ M) ranged from

90 to 390 nm in size ([Figure 3b](#)). Confocal microscopy showed that CaOx crystals were more aggregated and had an increased fluorescence signal compared to CaP crystals ([Figure 3c](#); black arrows denote crystals).

NTA Detects Urinary Nanocrystals in a Reproducible Manner

After confirming the feasibility of NTA to assess CaOx and CaP crystals, we tested whether urinary crystals could be detected by NTA. Pre-oxalate samples had crystals ranging between 75 and 300 nm in size (mean concentration, $7E+07 \pm 2.3E+07$ particles/ml; [Figure 4a](#) and [Table 2](#)), whereas post-oxalate samples were more dispersed and ranged from 100 to 400 nm in size (mean concentration, $4E+08 \pm 1.2E+08$ particles/ml; [Figure 4a](#) and [Table 2](#)). Notably, all pre-oxalate samples had some nanocrystals. We also detected an increased number of crystals in post-oxalate samples compared to pre-oxalate samples (black arrows denote crystals), which is compatible with the increased oxalate noted in [Table 1](#) and confocal microscopy ([Figure 4b](#)). Pre-oxalate and post-oxalate samples were measured in triplicate and showed reproducibility in both size and concentration ($20.3\% \pm 6.9\%$ coefficient of variance; [Supplementary Figure S3A](#) and [B](#)). In additional experiments, we tested whether urine samples stored at RT or 37 $^{\circ}$ C for 2 hours had any difference in signal with the NanoSight. We found that there was no change in crystal concentration, although small changes in crystal aggregation may have occurred as evidenced by the additional peaks ([Supplementary Figure S4](#)).

Crystalline Oxalate Correlates With Nano- and Micro-Crystals in Post-Oxalate Load Urine

As shown in [Figure 2b](#), crystalline urinary oxalate levels were significantly elevated following an oxalate load compared to pre-oxalate samples. The percentage of oxalate in nanocrystals was higher in post-oxalate samples versus pre-oxalate samples ($0.25\% \pm 0.07\%$

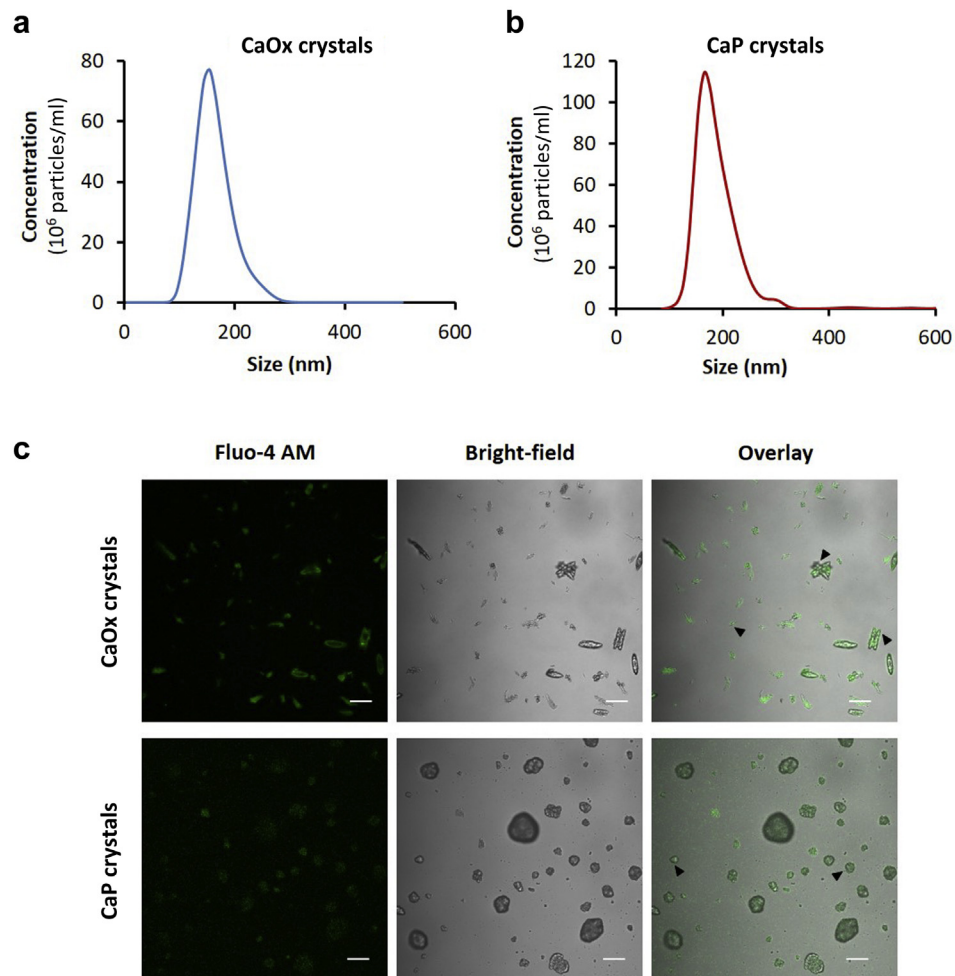


Figure 3. The detection of calcium oxalate (CaOx) and calcium phosphate (CaP) crystals using nanoparticle tracking analysis and confocal microscopy. Representative size distribution of (a) CaOx and (b) CaP crystals (50 μM) labelled with Fluo-4 AM (calcium probe) using nanoparticle tracking analysis. (c) Representative confocal microscopy images of CaOx and CaP crystals labelled with Fluo-4 AM (black arrows denote crystals; bars = 20 μm).

pre-oxalate vs. $0.60\% \pm 0.36\%$ post-oxalate). These values are only a small fraction of the total oxalate determined. The total number of nanocrystals detected by NTA positively correlated with crystalline oxalate levels ($R^2 = 0.75$) in post-oxalate urine samples (Figure 5). We did not see any direct correlation between nanocrystals and oxalate concentrations in urine.

Confirmation of Urinary Crystals Using Microscopy

Polarized light and electron microscopy were used to further assess urinary crystals. As mentioned above, polarized light microscopy is commonly used to detect CaOx crystals in urine samples. Both pre-oxalate and post-oxalate samples contained crystals that were birefringent (Figure 6a). Larger birefringent crystals were present in post-oxalate samples ($\sim 10\text{--}15\ \mu\text{m}$) compared to pre-oxalate samples ($\sim 2\text{--}8\ \mu\text{m}$). The

ability to visualize nanocrystals using polarized light microscopy was not possible as this method can only visualize micro-sized crystals. We used electron microscopy to evaluate whether nanocrystals existed in both pre-oxalate and post-oxalate samples (Figure 6b). Few nanocrystals were detected in pre-oxalate samples ($<200\ \text{nm}$). In contrast, post-oxalate samples contained more nanocrystals that were cylindrical, aggregated, larger in size ($>200\ \text{nm}$), and had a morphology similar to CaOx crystals.

Urinary Nanocrystal Composition Using FTIR and IC Analysis

Calcium can bind to oxalate and phosphate or be found in cellular debris. FTIR analysis was used to confirm the presence of oxalate and phosphate in urine crystalline samples. The FTIR spectrum of CaOx and CaP crystals showed characteristic absorption bands for oxalate at $1610\ \text{cm}^{-1}$, $1319\ \text{cm}^{-1}$, $780\ \text{cm}^{-1}$, and for

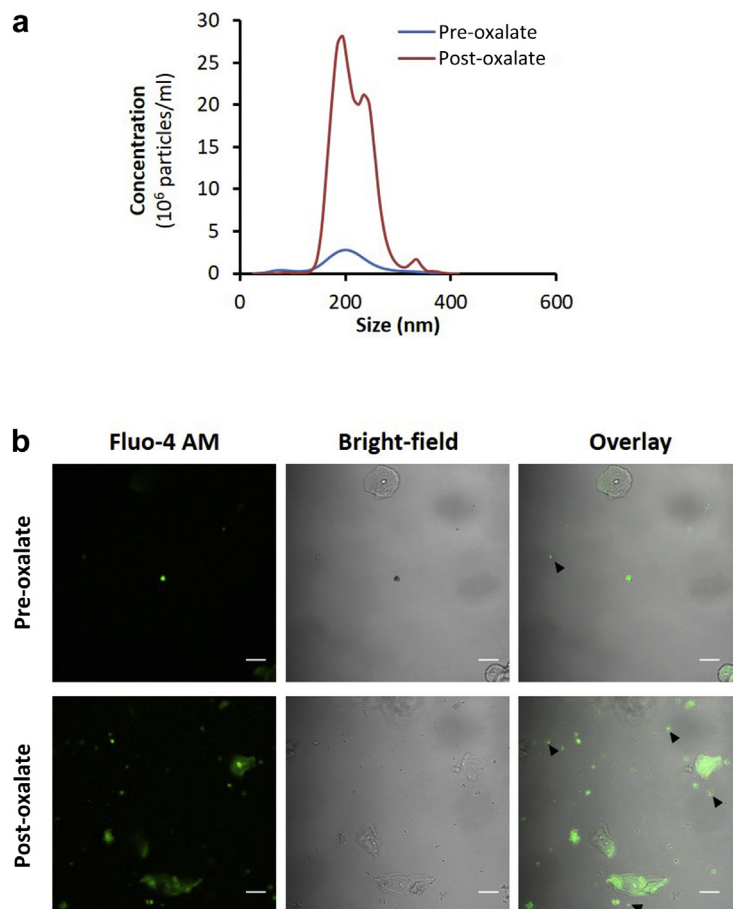


Figure 4. The detection of urinary crystals in a healthy subject on a controlled diet using nanoparticle tracking analysis and confocal microscopy. (a) Representative size distribution of urinary nanocrystals labelled with Fluo-4 AM in a healthy subject on a controlled diet before (pre-oxalate sample) and following an oxalate load (post-oxalate sample). (b) Representative confocal microscopy images of pre-oxalate and post-oxalate samples (black arrows denote crystals; bars = 20 μ m).

phosphate at 660 cm^{-1} and 561 cm^{-1} (Figure 7a). Pre-oxalate and post-oxalate load urine samples had similar absorption bands for oxalate and phosphate as CaOx and CaP crystals (Figure 7b). Calcium, oxalate, and phosphate levels were further quantified in ethanol-washed urinary pellets using IC and IC/MS. Both calcium and phosphate did not differ between pre-oxalate and post-oxalate samples (Table 2). The detection of calcium in the pre-oxalate load sample supports the presence of CaOx and CaP crystals. The increase in oxalate in the post-oxalate load samples is consistent with the increased number of CaOx crystals post-load (Table 2).

DISCUSSION

Although crystals are the building blocks of all stones, the role of urinary crystals in stone formation is not clear. It has been suggested that consuming meals rich in oxalate can result in crystalluria.⁴⁰ Increased urinary oxalate excretion can also increase stone risk by inducing renal tubule damage and disrupting protective urinary macromolecules.^{1,41,42} We and others have

shown that urinary crystals can impact cellular pathways in cultured renal cells and circulating immune cells.^{43–49} Conventional methods that have been used to detect urinary microcrystals include polarized light microscopy, scanning electron microscopy, X-ray diffraction, particle counting, urine filtration, evaporation, and centrifugation,^{9–14} but none of these have been used to quantify nanocrystals. Crystal size may also be an important factor in cell injury, as recent studies have shown that CaOx nanocrystals cause more cytotoxic effects than microcrystals on renal epithelial cells.²⁵ Furthermore, nano-scaled crystallites isolated from CaOx stone formers have been shown to more

Table 2. Oxalate, calcium, and phosphate levels in ethanol-washed urine pellets

	Pre-oxalate	Post-oxalate
Nanocrystals (particles/ml)	7E+07 \pm 2.3E+07	4E+08 \pm 1.2E+08
Oxalate (mg)	0.08 \pm 0.02	0.26 \pm 0.08
Calcium (mg)	1.4 \pm 0.4	2.2 \pm 0.8
Phosphate (mg)	320.5 \pm 115.6	323.8 \pm 100.5

Data are presented as mean \pm SEM.

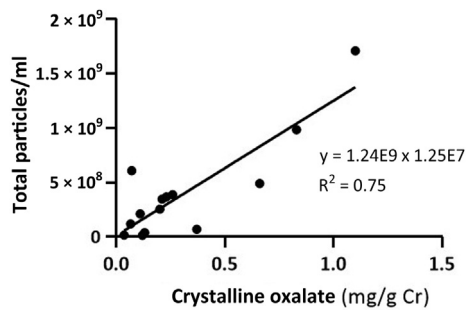


Figure 5. The relationship between urinary crystalline oxalate levels and the total number of post-oxalate urinary nanoparticles in healthy subjects on controlled diets. Correlation of the total number of urinary nanocrystals versus crystalline oxalate levels in post-oxalate samples from healthy subjects.

easily aggregate and agglomerate.²⁷ Thus, the ability to accurately detect nanocrystals in the urine could be a useful tool for identifying factors associated with crystal agglomeration and crystal toxicity, and for understanding and managing kidney stone disease.

Few studies have detected nanocrystals in the urine using a nanoparticle analyzer and nano-flow cytometer.^{14,27,28} These methods required labeling crystals with fluorescent probes and dyes for visualization under the microscope or flow cytometry.^{28,50} Their findings suggested nanocrystals could be important to understand stone pathogenesis. Limitations to this approach include lack of specificity of calcium or magnesium, instrument costs, and the need for high-level technical expertise.

We developed a sensitive method to evaluate urinary nanocrystals using a fluorescent dye and NTA. We further show urinary nanocrystals are observed in fasted healthy subjects on controlled diets (pre-oxalate samples) and that the number of urinary calcium oxalate crystals is increased following a dietary oxalate load. NTA using NanoSight technology has previously been used to detect nanoparticles in biological samples.^{30,32,51} Fluo-4 is a calcium-binding probe that was developed to detect free calcium in biological systems and has high fluorescence upon binding to calcium.^{35,52} It has been used to visualize calcium-containing microcrystals (calcium pyrophosphate dihydrate, basic CaP, hydroxyapatite, and CaOx) in synovial fluid from patients with arthritis using microscopy and flow cytometry,³⁵ and to calcify nanoparticles in feline urine.⁵¹ In our hands, crystals labelled with Fluo-4, Calcium green, or Calcein Ultragreen AM did not effectively detect nanocrystals using NTA. However, we were able to detect crystals using Fluo-4 AM, a membrane-permeable form of Fluo-4. The ability of this dye to specifically label nanocrystals could be due to its physical properties (e.g., charge). The inactivity of Calcein Ultragreen AM suggests that several factors

may be involved in producing the fluorescence associated with Fluo-4 AM binding. We also evaluated samples by light scattering without fluorescence labeling, and these results indicated that Fluo-4 AM yielded more-specific results than light scattering alone. We established that NTA can accurately and efficiently measure the size and concentration of nanocrystals in a dose-dependent and reproducible manner.

Urinary nanocrystals were also present in all pre-oxalate samples, and this could be due to urine supersaturation occurring in early-morning voided urine^{53,54} or the possibility of crystals remaining in the bladder following the first void of the day. There were more urinary crystals and greater crystal aggregation following the oxalate load compared to pre-oxalate samples. The nanocrystals observed (i.e., 100–300 nm) were consistent with another study that reported urinary crystallites from healthy subjects ranging from 100 to 350 nm in size.⁵⁵ A large proportion of crystals we observed were larger than urinary exosomes, which range from 20 to 100 nm.^{56,57} To ensure optimal measurements, we used a consistent camera level, detection threshold, focus, and flow rate, as each of these parameters could affect particle assessment.^{58–60} In particular, we used a flow rate of 20 $\mu\text{l}/\text{min}$. It has been shown previously that flow rate (i.e., $>50 \mu\text{l}/\text{min}$ or $<20 \mu\text{l}/\text{min}$) can affect the detection of particles.⁶¹ The coefficients of variance of our size estimates of crystals in urinary samples were consistent with the 4% coefficient of variance determined for the size of standard nanoparticles reported in another interlaboratory study.⁵⁸

To extend our knowledge of the particles we detected by NTA, we implemented confocal imaging, polarized light microscopy, electron microscopy, and FTIR analyses. Confocal microscopy revealed green fluorescence labelling of micron-sized crystals and was consistent with another study reporting crystals in synovial fluid.³⁵ These crystals were also birefringent under polarized light. Due to the limit of detection of confocal and polarized light microscopy, urinary nanocrystals were visualized using electron microscopy. The crystal size and morphology (e.g., cylindrical, spindle, and envelope) were similar to those in other reports characterizing CaOx monohydrate crystals with scanning electron microscopy.^{62,63} Notably, there were few dispersed nanocrystals in the pre-oxalate samples; there were more aggregated crystals in post-oxalate load samples. In a separate experiment, we found that the amount of crystals present in pre-oxalate samples was lower than in urine samples from healthy subjects not on a low-oxalate diet. We also observed some cellular debris in the samples,

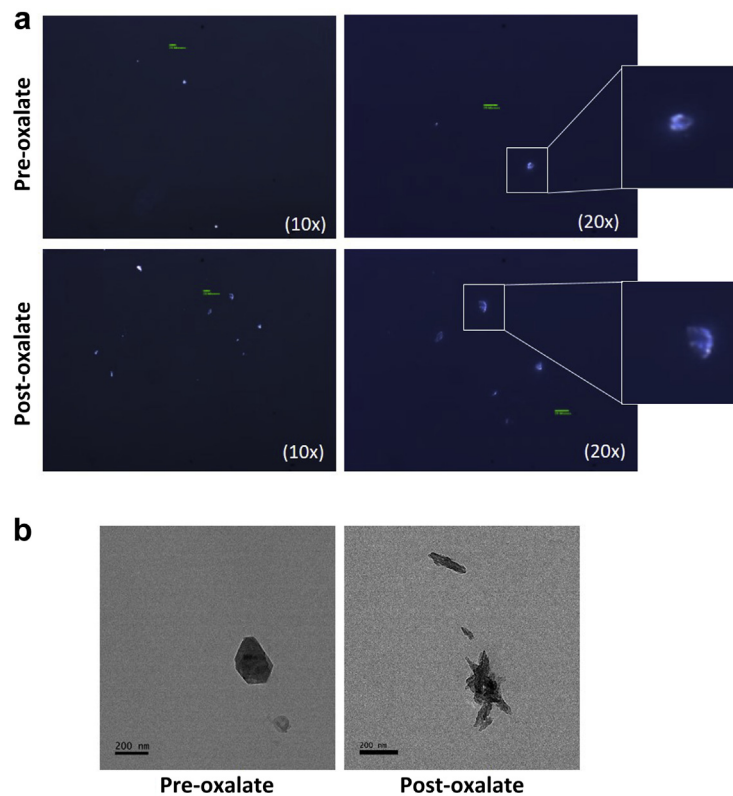


Figure 6. The detection of urinary crystals in pre-oxalate and post-oxalate samples using polarized light microscopy and electron microscopy. (a) Representative polarized light microscopy of pre-oxalate and post-oxalate samples (original magnification $\times 10$ and $\times 20$; bar = $20\ \mu\text{m}$). (b) Representative electron microscopy of pre-oxalate and post-oxalate samples (bars = $200\ \text{nm}$).

suggesting that other proteins, nucleic acids, or membranous material may be present. Additionally, $\sim 70\%$ of study participants had an increase in both urinary micro-sized and nano-sized crystals following the load.

As both CaOx and CaP can become supersaturated in urine,⁴¹ oxalate and phosphate concentrations were evaluated in this study. FTIR analysis indicated that crystals were indeed comprised of both oxalate and phosphate, and these findings were consistent with a study examining oxalate and phosphate using FTIR in CaOx, CaP, and mixed stones from humans.⁶⁴ However, IC analysis showed that the phosphate concentration was much higher than that of calcium or oxalate, and was not significantly different before versus after the oxalate load. The amount of phosphate present in these samples could be due to DNA, phospholipids, or phosphoproteins in cellular debris. Collectively, these findings indicate that NTA can successfully measure both CaOx and CaP urinary nanocrystals less than $1\ \mu\text{m}$ in size, but it cannot discriminate between them.

Some advantages of using NTA include the ability to quantify particles with and without fluorescence labelling. The potential of NTA to assess urinary CaOx and CaP nanocrystals could be useful to better understand the significance of crystalluria. It provides a

platform to comprehensively determine the size and number of crystals present in urine and could help define the pathophysiology of kidney stone formation. It also may have clinical utility as it could define kidney stone risk and response to preventive therapy or may have relevance in other medical conditions where crystals are involved. For example, it may be useful in chronic kidney disease, as oxalate excretion has been shown to correlate with chronic kidney disease progression.⁶⁵ Strengths of this method include minimal variability amongst (i) samples on a day-to-day basis and (ii) the size of urinary nanocrystals and CaOx crystals. Some limitations of the study include (i) the inability to distinguish between CaOx monohydrate, CaOx dihydrate crystals, CaP crystals, and other potential crystals; (ii) nonassessment of nanocrystal morphology; and (iii) the inability to determine where crystals form in the urinary tract. Based on our data, it appears nanocrystals may be forming in the renal tubules rather than the bladder, based on diuresis in post-oxalate load samples. Additional studies using experimental models are required to confirm such hypotheses.

Overall, the current study demonstrates that NTA can quantify urinary nanocrystals, including those generated after a dietary oxalate load. The findings

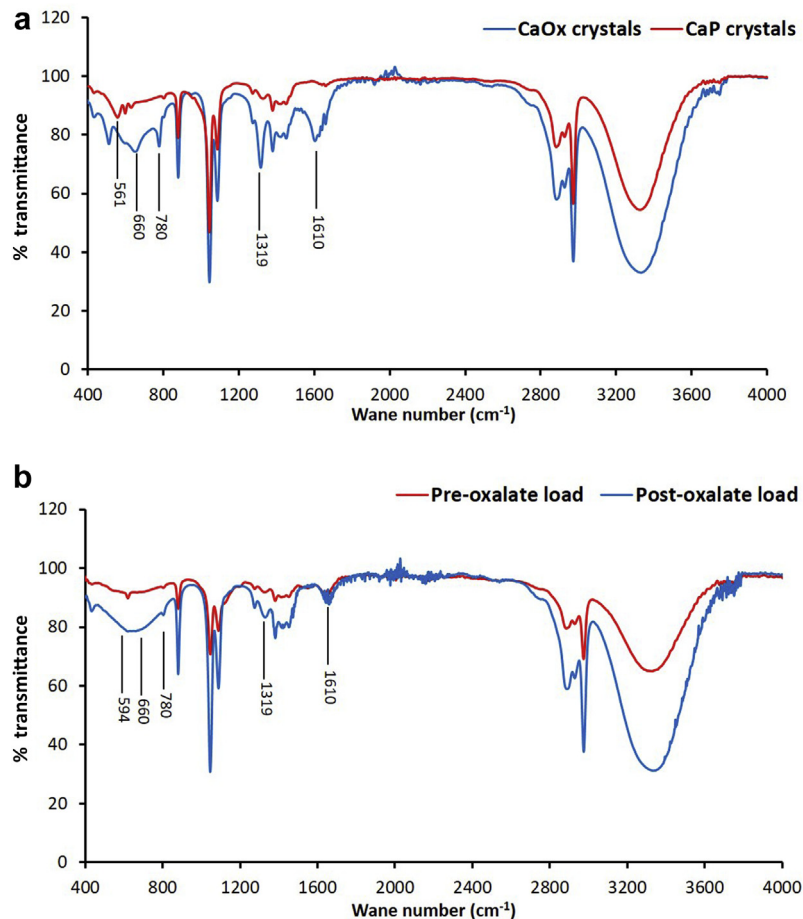


Figure 7. Characterization of crystals using Fourier transform infrared spectroscopy analysis. Representative % transmittance of (a) calcium oxalate (CaOx) and calcium phosphate (CaP) crystals and (b) pre-oxalate and post-oxalate urinary crystals.

from this study provide some insight regarding the role of nanocrystals in crystallite and kidney stone formation. Additional questions that arise from this study include: Is there a difference in the concentration and size of nanocrystals in stone formers compared to non-stone formers? Why and how does Fluo-4 AM bind specifically to urinary CaOx crystals? Are there crystal nucleation sites within the nephron on the cell surface, and if so, what is the condition of the fluid phase? What are the effects of these nanocrystals on kidney function and the immune system? We plan to explore these queries in the future using animal studies and translational studies in humans.

DISCLOSURE

All the authors declared no competing interests.

DATA STATEMENT

Due to the sensitive nature of this study, participants were assured raw data would remain confidential and would not be shared.

ACKNOWLEDGMENTS

We thank all study subjects for their participation. We also acknowledge Dr. Kasturi Mitra and Danitra Parker for assistance with confocal microscopy; Dr. Dezhi Wang for assistance with polarized light microscopy (UAB Pathology Core Research Laboratory); Dr. Terje Dokland and Cynthia M. Rodenburg for assistance with electron microscopy (UAB Cryo-EM facility, Center for Structural Biology); and Dr. Edward Inscho for scientific discussion. This work was supported by National Institutes of Health grants DK106284 (TM), DK079337 (UAB O'Brien Center), and UL1TR001417 (National Center for Advancing Translational Sciences).

SUPPLEMENTARY MATERIAL

[Supplementary File \(PDF\)](#)

Figure S1. The detection of urinary crystals using fluorescence dyes.

Figure S2. The detection of CaOx crystals at various concentrations using nanoparticle tracking analysis (NTA).

Figure S3. Technical replicates of samples using nanoparticle tracking analysis (NTA).

Figure S4. The effects of temperature on urinary crystals using nanoparticle tracking analysis (NTA).

REFERENCES

- Mitchell T, Kumar P, Reddy T, et al. Dietary oxalate and kidney stone formation. *Am J Physiol Renal Physiol.* 2019;316:F409–F413.
- Worcester EM, Coe FL. Clinical practice. Calcium kidney stones. *N Engl J Med.* 2010;363:954–963.
- Coe FL, Parks JH, Asplin JR. The pathogenesis and treatment of kidney stones. *N Engl J Med.* 1992;327:1141–1152.
- Kuo RL, Lingeman JE, Evan AP, et al. Urine calcium and volume predict coverage of renal papilla by Randall's plaque. *Kidney Int.* 2003;64:2150–2154.
- Evan AP, Lingeman JE, Coe FL, et al. Randall's plaque of patients with nephrolithiasis begins in basement membranes of thin loops of Henle. *J Clin Invest.* 2003;111:607–616.
- Williams JC Jr, Borofsky MS, Bledsoe SB, et al. Papillary ductal plugging is a mechanism for early stone retention in brushite stone disease. *J Urol.* 2018;199:186–192.
- Uvarov V, Popov I, Shapur N, et al. X-ray diffraction and SEM study of kidney stones in Israel: quantitative analysis, crystallite size determination, and statistical characterization. *Environ Geochem Health.* 2011;33:613–622.
- Ghosh S, Bhattacharya A, Chatterjee P, Mukherjee Alok K. Structural and microstructural characterization of seven human kidney stones using FTIR spectroscopy, SEM, thermal study and X-ray Rietveld analysis. *Zeitschr. Kristallogr. Crystall. Mat.* 2014;229:451–458.
- Hallson PC, Rose GA. A new urinary test for stone "activity." *Br J Urol.* 1978;50:442–448.
- Bader CA, Chevalier A, Hennequin C, et al. Methodological aspects of spontaneous crystalluria studies in calcium stone formers. *Scan Microsc.* 1994;8:215–231; discussion 231–212.
- Werness PG, Bergert JH, Lee KE. Urinary crystal growth: effect of inhibitor mixtures. *Clin Sci (Lond).* 1981;61:487–491.
- Fan J, Chandhoke PS. Examination of crystalluria in freshly voided urines of recurrent calcium stone formers and normal individuals using a new filter technique. *J Urol.* 1999;161:1685–1688.
- Robertson WG, Peacock M, Nordin BE. Calcium crystalluria in recurrent renal-stone formers. *Lancet.* 1969;2:21–24.
- He JY, Deng SP, Ouyang JM. Morphology, particle size distribution, aggregation, and crystal phase of nanocrystallites in the urine of healthy persons and lithogenic patients. *IEEE Trans Nanobiosci.* 2010;9:156–163.
- Werness PG, Bergert JH, Smith LH. Crystalluria. *J Crystal Growth.* 1981;53:166–181.
- Frochot V, Daudon M. Clinical value of crystalluria and quantitative morphoconstitutional analysis of urinary calculi. *Int J Surg.* 2016;36:624–632.
- Daudon M, Frochot V, Bazin DPJ. Crystalluria analysis improves significantly etiologic diagnosis and therapeutic monitoring of nephrolithiasis. *Comptes Rendus Chimie.* 2016;19:1514–1526.
- Holmes RP, Ambrosius WT, Assimos DG. Dietary oxalate loads and renal oxalate handling. *J Urol.* 2005;174:943–947; discussion 947.
- Knight J, Holmes RP, Assimos DG. Intestinal and renal handling of oxalate loads in normal individuals and stone formers. *Urol Res.* 2007;35:111–117.
- Shapur NK, Uvarov V, Popov I, et al. Crystallite size—is it a new predictor for renal stone burden? *Urology.* 2012;80:980–985.
- Prochaska M, Taylor E, Ferraro PM, Curhan G. Relative supersaturation of 24-hour urine and likelihood of kidney stones. *J Urol.* 2018;199:1262–1266.
- Evan AP, Worcester EM, Coe FL, et al. Mechanisms of human kidney stone formation. *Urolithiasis.* 2015;43(suppl 1):19–32.
- Dorian HH, Rez P, Drach GW. Evidence for aggregation in oxalate stone formation: atomic force and low voltage scanning electron microscopy. *J Urol.* 1996;156:1833–1837.
- Mulay SR, Anders HJ. Crystallopathies. *N Engl J Med.* 2016;374:2465–2476.
- Sun XY, Ouyang JM, Yu K. Shape-dependent cellular toxicity on renal epithelial cells and stone risk of calcium oxalate dihydrate crystals. *Sci Rep.* 2017;7:7250.
- Khan SR. Reactive oxygen species as the molecular modulators of calcium oxalate kidney stone formation: evidence from clinical and experimental investigations. *J Urol.* 2013;189:803–811.
- Gao J, Xue J-F, Xu M, et al. Comparison of physicochemical properties of nano- and micro-sized crystals in the urine of calcium oxalate stone patients and control subjects. *J Nanomater.* 2014;2014:9.
- Gavin CT, Ali SN, Taily T, et al. Novel methods of determining urinary calculi composition: petrographic thin sectioning of calculi and nanoscale flow cytometry urinalysis. *Sci Rep.* 2016;6:19328.
- Filipe V, Hawe A, Jiskoot W. Critical evaluation of nanoparticle tracking analysis (NTA) by NanoSight for the measurement of nanoparticles and protein aggregates. *Pharma Res.* 2010;27:796–810.
- Dragovic RA, Gardiner C, Brooks AS, et al. Sizing and phenotyping of cellular vesicles using Nanoparticle Tracking Analysis. *Nanomedicine.* 2011;7:780–788.
- Dragovic RA, Collett GP, Hole P, et al. Isolation of syncytiotrophoblast microvesicles and exosomes and their characterisation by multicolour flow cytometry and fluorescence Nanoparticle Tracking Analysis. *Methods.* 2015;87:64–74.
- Gercel-Taylor C, Atay S, Tullis RH, et al. Nanoparticle analysis of circulating cell-derived vesicles in ovarian cancer patients. *Anal Biochem.* 2012;428:44–53.
- Martin C, Patel M, Williams S, et al. Human breast milk-derived exosomes attenuate cell death in intestinal epithelial cells. *Innate Immun.* 2018;24:278–284.
- Carnell-Morris P, Tannetta D, Siupa A, et al. Analysis of extracellular vesicles using fluorescence nanoparticle tracking analysis. *Methods Mol Biol.* 2017;1660:153–173.
- Hernandez-Santana A, Yavorsky A, Loughran ST, et al. New approaches in the detection of calcium-containing microcrystals in synovial fluid. *Bioanalysis.* 2011;3:1085–1091.
- Ryall RL, Grover PK, Thurgood LA, et al. The importance of a clean face: the effect of different washing procedures on the association of Tamm-Horsfall glycoprotein and other urinary proteins with calcium oxalate crystals. *Urol Res.* 2007;35:1–14.

37. Fargue S, Milliner DS, Knight J, et al. Hydroxyproline metabolism and oxalate synthesis in primary hyperoxaluria. *J Am Soc Nephrol.* 2018;29:1615–1623.
38. Li X, Ellis ML, Dowell AE, et al. Response of germ-free mice to colonization with *O. formigenes* and altered Schaedler flora. *Appl Environ Microbiol.* 2016;82:6952–6960.
39. Dokland T, Hutmacher DW, Ng MM-L, Schantz J-T. *Techniques in Microscopy for Biomedical Applications.* Vol. 22006.
40. Fogazzi GB. Crystalluria: a neglected aspect of urinary sediment analysis. *Nephrol Dial Transplant.* 1996;11:379–387.
41. Khan SR, Kok DJ. Modulators of urinary stone formation. *Front Biosci.* 2004;9:1450–1482.
42. Balcke P, Zazgornik J, Sunder-Plassmann G, et al. Transient hyperoxaluria after ingestion of chocolate as a high risk factor for calcium oxalate calculi. *Nephron.* 1989;51:32–34.
43. Lieske JC, Toback FG. Interaction of urinary crystals with renal epithelial cells in the pathogenesis of nephrolithiasis. *Semin Nephrol.* 1996;16:458–473.
44. Patel M, Yarlagaadda V, Adedoyin O, et al. Oxalate induces mitochondrial dysfunction and disrupts redox homeostasis in a human monocyte derived cell line. *Redox Biol.* 2018;15:207–215.
45. Khan SR. Role of renal epithelial cells in the initiation of calcium oxalate stones. *Nephron Exp Nephrol.* 2004;98:e55–e60.
46. Mulay SR, Kulkarni OP, Rupanagudi KV, et al. Calcium oxalate crystals induce renal inflammation by NLRP3-mediated IL-1 β secretion. *J Clin Invest.* 2013;123:236–246.
47. Umekawa T, Chegini N, Khan SR. Oxalate ions and calcium oxalate crystals stimulate MCP-1 expression by renal epithelial cells. *Kidney Int.* 2002;61:105–112.
48. Huang MY, Chaturvedi LS, Koul S, Koul HK. Oxalate stimulates IL-6 production in HK-2 cells, a line of human renal proximal tubular epithelial cells. *Kidney Int.* 2005;68:497–503.
49. Liu Z, Wang T, Yang J, et al. Calcium oxalate monohydrate crystals stimulate monocyte chemoattractant protein-1 and transforming growth factor β 1 expression in human renal epithelial cells. *Mol Med Rep.* 2012;5:1241–1244.
50. Chaiyarit S, Mungdee S, Thongboonkerd V. Non-radioactive labelling of calcium oxalate crystals for investigations of crystal-cell interactions and internalization. *AnalytMeth.* 2010;2:1536–1541.
51. Mellema M, Stoller M, Queau Y, et al. Nanoparticle tracking analysis for the enumeration and characterization of mineralo-organic nanoparticles in feline urine. *PLoS One.* 2016;11:e0166045.
52. Minta A, Kao JP, Tsien RY. Fluorescent indicators for cytosolic calcium based on rhodamine and fluorescein chromophores. *J Biol Chem.* 1989;264:8171–8178.
53. Ahlstrand C, Larsson L, Tiselius HG. Variations in urine composition during the day in patients with calcium oxalate stone disease. *J Urol.* 1984;131:77–81.
54. Kok DJ, Khan SR. Calcium oxalate nephrolithiasis, a free or fixed particle disease. *Kidney Int.* 1994;46:847–854.
55. Gui BS, Huang ZJ, Xu XJ, et al. Measurement of urine crystallites and its influencing factors by nanoparticle size analyzer. *J Nanosci Nanotechnol.* 2010;10:5232–5241.
56. Erdbrugger U, Le TH. Extracellular vesicles in renal diseases: more than novel biomarkers? *J Am Soc Nephrol.* 2016;27:12–26.
57. Oosthuyzen W, Sime NE, Ivy JR, et al. Quantification of human urinary exosomes by nanoparticle tracking analysis. *J Physiol.* 2013;591:5833–5842.
58. Hole P, Silience K, Hannell C, et al. Interlaboratory comparison of size measurements on nanoparticles using nanoparticle tracking analysis (NTA). *J Nanopart Res.* 2013;15:2101.
59. Maas SL, de Vrij J, van der Vlist EJ, et al. Possibilities and limitations of current technologies for quantification of biological extracellular vesicles and synthetic mimics. *J Contr Release.* 2015;200:87–96.
60. Tomlinson PR, Zheng Y, Fischer R, et al. Identification of distinct circulating exosomes in Parkinson's disease. *Ann Clin Transl Neurol.* 2015;2:353–361.
61. Tong M, Brown OS, Stone PR, et al. Flow speed alters the apparent size and concentration of particles measured using NanoSight nanoparticle tracking analysis. *Placenta.* 2016;38:29–32.
62. Sun XY, Xu M, Ouyang JM. Effect of crystal shape and aggregation of calcium oxalate monohydrate on cellular toxicity in renal epithelial cells. *ACS Omega.* 2017;2:6039–6052.
63. Gan QZ, Sun XY, Ouyang JM. Adhesion and internalization differences of COM nanocrystals on Vero cells before and after cell damage. *Mater Sci Eng C Mater Biol Appl.* 2016;59:286–295.
64. Ma RH, Luo XB, Li Q, Zhong HQ. The systematic classification of urinary stones combine-using FTIR and SEM-EDAX. *Int J Surg.* 2017;41:150–161.
65. Waikar SS, Srivastava A, Palsson R, et al. Association of urinary oxalate excretion with the risk of chronic kidney disease progression. *JAMA Intern Med.* 2019;179:542–551.